MODELING AND CONTROL OF WIND AND ELECTRIC VEHICLES FOR FREQUENCY REGULATION IN A LARGE POWER SYSTEM

GANJI PRIYANKA[1], G.VANI[2]
[1]PG Student, Dept of EEE (PS), SITE, Tirupati, AP, India.
[2]Assistant Professor, Dept of EEE, SITE, Tirupati, AP, India.

ABSTRACT: The future smart grids are expected to include a high penetration of distributed generations (DGs), most of which will consist of renewable energy sources, such as solar or wind energy. It is believed that the high penetration of DGs will result in the reduction of power losses, voltage profile improvement, meeting future load demand, and optimizing the use of non-conventional energy sources. Wind generators and plug-in hybrid electric vehicles (PHEVs) are increasing rapidly in modern power grids. Despite all their merits, these two classes of sources are limited by some practical constraints which disqualify each of them from effectively contributing separately to the primary frequency regulation in power grids with reduced inertia, such as microgrids. However, when combined with proper control and coordination, wind generators and PHEVs can compensate for the individual drawbacks of each source and effectively participate in the frequency regulation.

Cooperative control makes it possible to organize different agents in a networked system to act as a group and realize the designated objectives. Cooperative control has been already applied to the autonomous vehicles and this work investigates its application in controlling the DGs in a micro grid. A cooperative control strategy that considers the practical limits of both sources is not available in the literature. To fill this gap, in this study, small signal analysis is employed to investigate which frequency regulation method, droop or virtual inertia, is more suitable for such cooperation. The centralized and distributed control structures are examined as two possible coordination methods to ensure that the wind generator and PHEVs constraints are not violated and also that the communication system delay is considered. MATLAB/SIMULINK simulation results, obtained by using a typical microgrid system, validate the analytical results.

I. INTRODUCTION

The requirements to enable an active EV participation with the power system are defined. The interaction between the EVs and the grid should involve a safe bidirectional EV battery operation. An experimental EV setup is built using full scale EV components to assess the EV system response under an EV coordination concept. An EV's control architecture is developed to enable the EVs for the provision of ancillary services within a centralized coordination concept of a Virtual Power Plant. Considering the simplified LV distribution feeder of figure 1, the goal is to propose methodologies for the coordination of EV load, to provide voltage regulation in a feeder, during periods of high PV generation and low consumption.

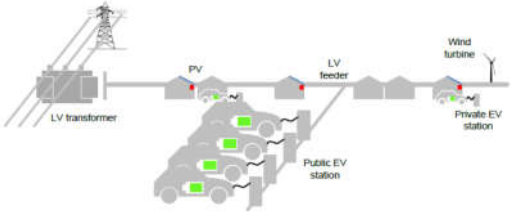

Fig:1. EV charging infrastructures in a LV distribution grid.

In different countries in Europe, the increasing wind power and PV installed capacity has set high requirements on power balance control as well as on power quality. Large off-shore wind farms concentrate a high power capacity at a single location. Due to the wind speed variations, the magnitude of the power fluctuations can reach very high values. The 10-minute average wind power profile from the 160 MW wind farm Horns Rev, is depicted. Over the 11-day period, the normalized wind power production varies from zero to almost 100% production. Wind power fluctuations are visible at different time-scales, short (intra-hour) and long (several hours). Also PV has in common that the active power production is variable over time; this aspect makes wind power and PV non-dispatchable energy sources. The Transmission System Operator (TSO) has the challenging task to ensure the balance between consumption and production, at all times, including at intra hour time scales. To facilitate the integration of RES in the power system, the research has focused on the potential contribution of EVs. The topic has been developed within the paradigm of *smart grid* and it is centred on the EV's potential of creating mutual benefits to both the electric power system with RES and future EV users. With the term *smart grid* is meant the operation of the power system using

communication and control technology, power electronics technologies and storage technologies to balance production and consumption at all levels.

II. SYSTEM MODELING

The PHEVs are fast power sources; however, their available energy for frequency regulation is limited. On the other hand, wind generators are rich sources of energy, but fast interactions can result in their fatigue. These characteristics make these two sources great choices to complement each other. Therefore, the droop or the virtual inertia can be used by a centralized controller to decide how much power is needed to regulate the power system frequency, and then, the same control center can divide the power between these two sources based on their individual characteristics. The structure of the centralized controller is depicted in Fig.2. The controller gathers information from the microgrid, PHEVs and wind generator and sends back commands to the sources. As discussed in low-pass filter (LPF) can be employed to share the power, but the coordination in practice is not straightforward because the energy storages units of the PHEVs are distributed and dispersed.

For a meaningful analysis, a detailed model is needed. The system depicted in Fig. 3 is adopted in this paper. The system is a typical medium-voltage rural distribution system, a real system in Ontario, Canada. The segment after the circuit breaker B2 can operate in the islanded mode and constitute a microgrid. It contains two DG units. DG1 is a variable-speed wind turbine connected to a 2.5 MVA PMSG with a full-scale converter. DG2 is a 2.5 MVA synchronous generator with droop and excitation control systems. The system parameters are given in the Appendix. The stability analysis can be extended to either larger microgrids or weak grids.

A small-signal model of a wind generator for frequency regulation dynamics is developed. To avoid repetition, the procedure of linearizing around an operating point, which is a function of the wind speed, is omitted here. The final results are presented in where *Δxw* represents the doubly-mass wind generator and its controller states. *Δvw* is the change in the wind speed, and *ΔPf* is the change in the power needed for frequency regulation; both are the inputs to this state-space representation. *ΔPw*, the output of the model, is the active power of the wind generator injected into the power system.

Based on the discussions on primary frequency regulation dynamics, the frequency dynamics of the microgrid system can be presented by the block diagram shown in Fig. 4. The traditional parts of the model, the turbine, the governor and the diesel rotating-mass, are described in detail in the literature.

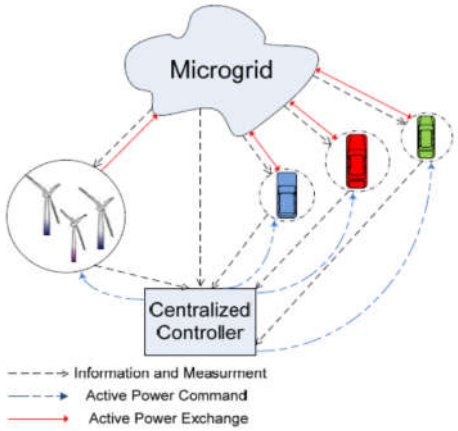

Fig. 2. Schematic view of the centralized controller.

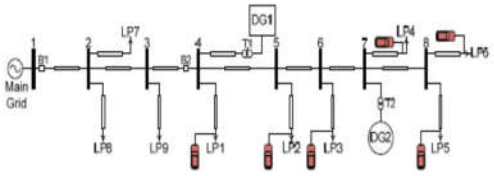

Fig. 3. System under study.

The wind generator and the PHEV and the proposed centralized controller are added here to the classical model to incorporate these modern components of power systems. As indicated in Fig. 4, the centralized controller decides how to respond to the frequency fluctuation. The command power is denoted as *ΔPreg*. It can be either the virtual inertia or the droop, formulated respectively. *Mv*, the virtual inertia gain, and *mp*, the droop gain, are the main levers used to control the contribution of the centralized controller to the frequency regulation dynamics. *Tc* is the time constant of the centralized controller.

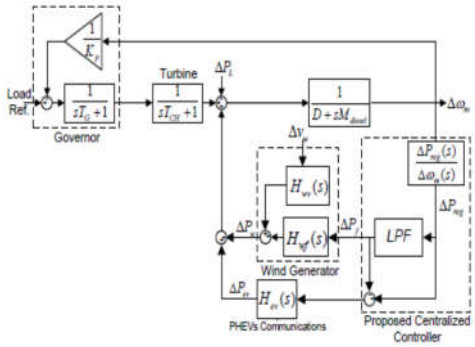

Fig. 4. Block diagram representation of the microgrid frequency dynamics with a centralized controller.

In fact, it represents the time constant of PHEVs' inverters and the grid side converter of the PMSG. As discussed in the literature, this time

constant is expected to be small. Then, an LPF extracts the low-frequency content, which will be communicated to the wind generator, *ΔPf*. The high frequency regulation command is communicated to PHEVs parking lots and aggregators. Electric vehicles are aggregated in one block in Fig. 4; however, the model can be easily modified to accommodate each parking lot or aggregator as one separate block.

A. IDEAL CASE

A perfect communication system is immune against any delay. Although such a system does not exist in reality, studying this situation is very enlightening. The maximum frequency deviation when the droop or the virtual inertia is employed. Obviously, the filter cutoff frequency has no impact, and only the frequency regulation gains, *mp* or *Mvi*, are determining. On the other hand, both the frequency regulation method and the filter can impact the stress on the wind generator shaft. To better understand the situation, where the maximum torque and the maximum rate of change of torque (ROCOT) of the wind generator shaft are depicted. Reference discussed in detail that the shaft fatigue is a function of the torque shaft and its derivative. In fact, the cutoff frequency of the LPF used in the centralized controller can play a vital role in relieving the mechanical tension of wind generators. The mechanical tension on the turbine shaft will be reduced by lowering the filter cutoff frequency because a larger portion of energy is provided by the PHEVs energy storages. This fact can be understood by observing the blue solid curves. Thus, the main tradeoff is between using more energy from the PHEVs batteries and putting more tension on the turbine shaft. PHEVs energy has a close relation with their state of charge, as discussed. The less the energy fed by PHEVs, the less their SOCs will change. However, the behavior patterns of the droop and virtual inertia methods are not the same. The red dashed curves in represent the maximum energy and power extracted from the combined hybrid source (wind generator and PHEVs together). As can be expected, they do not change significantly by changing the filter cutoff frequency. In other words, the LPF does not influence the external behavior of the combination but manages the behavior of the wind generator and PHEVs. Both the virtual inertia and the droop provide almost all the needed energy and power from PHEVs as the filter cutoff frequency converges to zero.

However, in the case of the droop method, the share of the PHEVs drops very rapidly by deviating from zero and then saturates. This fast deviation provides the chance to choose a cutoff frequency that mitigates mechanical tensions on the wind turbine shaft significantly, whereas the largest share of energy still comes from the wind generator, not the vehicles storages. The situation becomes clearer when the droop case is compared to the virtual inertia one. In fact, the difference is even more severe than what these figures show because the time frame used in them is just the first ten seconds right after the disturbance. While the virtual inertia usually settles to zero in this time frame, the droop method continues to provide power and energy for the power system until the secondary regulation restores the system frequency to its nominal value. The secondary control is usually activated 30 s to one minute after the disturbance and may take several minutes to regulate the system frequency.

More information on the secondary frequency regulation can be found. This difference leads to questioning the benefits of the coordinated virtual inertia for the PHEVs, even though it reduces the wind generator fatigue. The burden of communication and coordination is also added to the system. For this reason, the droop will be used as the main tool for the frequency regulation by the coordinated sources in the rest of this paper. From the power extraction perspective, both the virtual inertia and the droop method act similarly. No fast fall, similar to the droop energy extraction, can be observed here. However, the PHEVs are fast sources and have no difficulty injecting active power unless it changes their SOC significantly or exceeds their inverter rating.

In fact, it can be used to find out the number of vehicles needed for cooperative frequency regulation. One per unit power in this study is equal to the nominal rating of the synchronous generator, DG2, and is equivalent to 313 to 380 vehicles. The curves are obtained when the system is responding to a disturbance of 1.0 pu. Due to the linear nature of the analyses, the response to any other amount of disturbance can be calculated by using a simple scaling. By choosing the filter cutoff frequency 0.1 Hz, less than 245 vehicles are needed to respond to 1.0 pu disturbance. These vehicles in total inject less than 0.2 kWh maximally. This amount of energy is less than two percent of one battery capacity in common vehicles. Considering the number of involved vehicles, the SOC of their batteries will not be significantly changed. This result is desirable for the PHEVs owners. However, the vehicles will provide a large amount of power for the system. In other words, the PHEVs in the proposed coordination are used as the power sources rather than the energy sources. In this categorization of sources, power sources provide a high amount of power in a relatively short period so that the total supplied energy is not significant. In contrast, energy sources do not inject a high amount of power in a short period, but the amount of energy supplied in longer periods is significant.

B. DELAY

Assuming an ideal communication system is helpful for understanding some major characteristics of the proposed coordinated control; however, practical communication systems are not ideal. Therefore, the impact of the communication delay is considered in this study. This new model is used to find out the impact of the communication delay on the system stability. The maximum delay which does not destabilize the power system. The calculations of the maximum delay are based on the very popular concepts of small-signal analyses and root locus. In short, in the system shown in Fig. 4, the delay is increased in very small steps, and each time, the poles of the system are calculated. As long as whole poles are in the left half plane, the system is stable, and consequently, the corresponding delay is allowed. However, by increasing the delay, some poles start to move toward the right-half plane. The maximum allowable delay occurs when all the poles are still in the left-half plane, and a slight increase of the delay leads to instability.

This figure reveals that in low contributions of the PHEVs to the frequency regulation, i.e., relatively small *mp* or *Mvi*, the system is very robust against delays. However, it does not perform similarly when these sources play larger roles in the system frequency regulation. The situation is very similar for both the virtual inertia and droop methods. The model may be criticized for using one single delay for all PHEVs after they have been clustered by several parking lots and aggregators. To check this point, the PHEVs block was split into several blocks with unequal delays. It was found that if the average delay of these units exceeds the maximum allowable delay, the system becomes unstable.

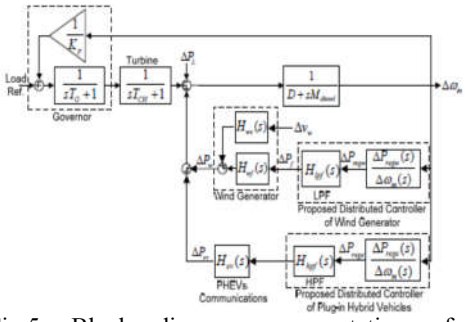

Fig.5. Block diagram representation of the microgrid frequency dynamics with a distributed cooperative controller.

Unlike the systems in Figs. 2 and 4, no central unit is employed in the system in Fig.5. The frequency is measured locally and fed into the local droop blocks. The generated reference power needed for the frequency regulation goes through an LPF or a high-pass filter (HPF) before reaching the wind and the PHEVs parking lots, respectively. Ideally, the system acts exactly like the perfect centralized controller. However, achieving such an ideal situation in reality is, if not impossible, rare. First of all, a delay could still exist. However, thanks to the distributed controller, the delays can be reduced dramatically with local measurements. Our studies showed that delays of less than 20 ms had no significant impact even in the case of high contributions from the wind generator and PHEVs. Smart parking lots or aggregators in dense areas can easily communicate with their vehicles with such small delays via low-cost local networks, which already exist for billing and monitoring. However, as discussed in the following subsection, the distributed coordination scheme is subject to some other unique threats and opportunities. Because the power system is subject to continuous changes and no immediate direct communication occurs between the PHEVs and the wind generator, the proposed controller must be robust against miscoordination and provide accessible control leverages.

III. SIMULATION RESULTS

Detailed nonlinear MATLAB/Simulink simulations, using the microgrid system shown in Figure, are used to verify the results of the pervious sections and investigate the nonlinear dynamics of the microgrid system. Typical distribution system lines, with a low *X*/*R* ratio (*X*/*R* =2), are modeled as lumped RL whereas loads are modeled by parallel *R*-*L* circuits. An intentional islanding event at *t*=0.2 s is used as the disturbance for the system.

CASE-A: CENTRALIZED COORDINATION

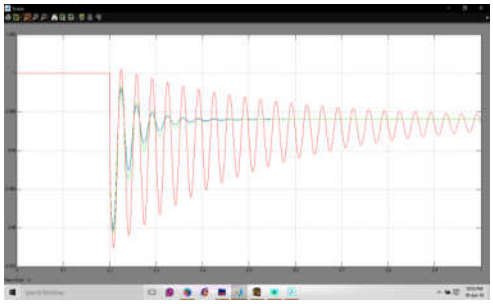

Fig:6(a) freq(p.u)

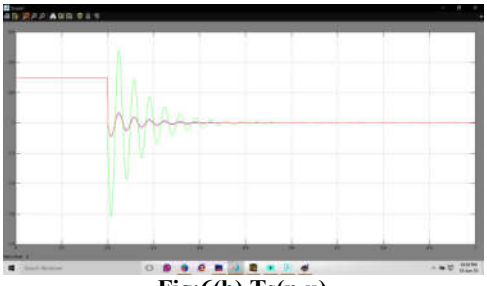

Fig:6(b) Ts(p.u)

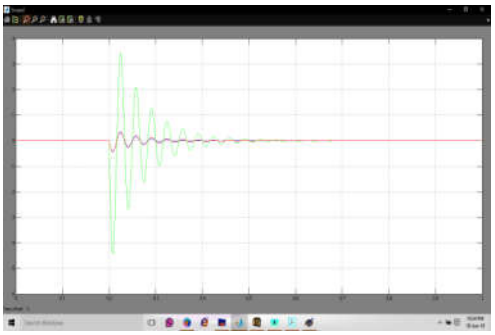

Fig:6(c) ROCOTs(pu)

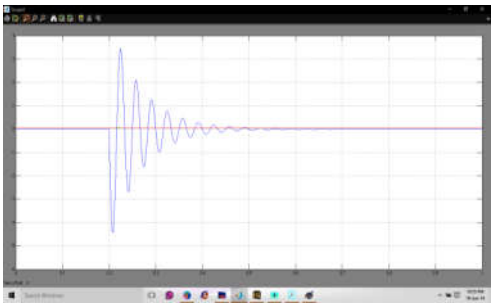

Fig:6(d) Pev(pu)

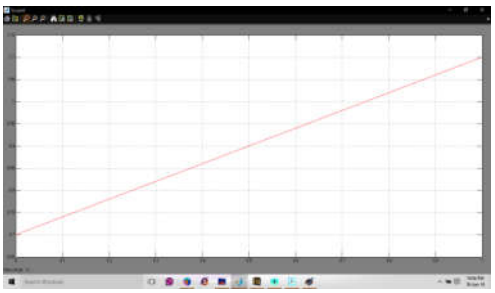

Fig:6(e) Eev(Kwh)

Fig. 6. simulation waveforms of Centralized control performance.

Fig. 6 shows the system performance when a centralized coordination is used. The ideal and no compensation cases refer to perfect communication and wind-only frequency regulating situations, respectively. Figs. 6(b) and 6(c) verify that the coordinated control is successful in mitigating the mechanical tensions on the turbine shaft and figures (d) and (e), supporting the argument of the previous section that the PHEVs are used as power sources, not energy ones. The energy restored in PHEVs restores to its ideal amount very fast. This fast restoration shows that the SOC of the battery restores to its desired amount in a few seconds. To provide the power needed from PHEVs, 31 to 38 vehicles are needed to operate at their rating power. On the other hand, the maximum deviation from the energy stored in the wind-only case is less than 0.02 kWh in total. In other words, on average, each vehicle's battery should supply less than 0.004% of its nominal capacity to frequency regulation. This small energy consumption means that the change in the charge state of the vehicles is negligible even though have provided a significant amount of vital power for the power system stabilization. The impact of communication delays is also shown in this figure. The yellow dashed curve in Fig. 6(a) shows that a delay as small as 75 ms will put the whole system at the verge of instability.

CASE-B: DISTRIBUTED COORDINATION

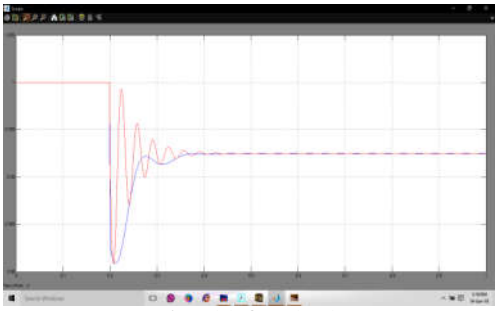

Fig:7(a) freq(p.u)

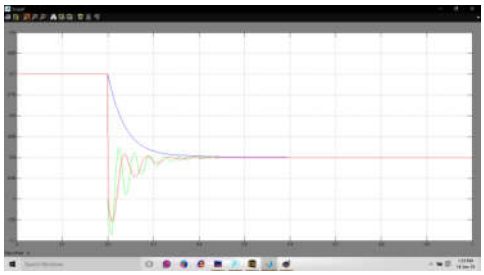

Fig:7(b) Ts(p.u)

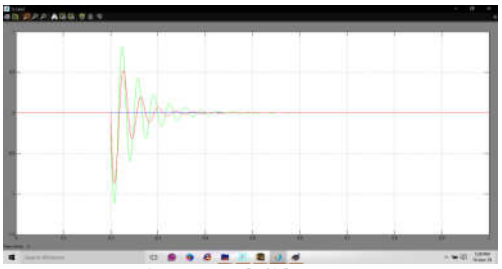

Fig:7(c) ROCOTs(pu)

Fig:7(d) Pev(pu)

Fig:7. Simulation waveforms of Impact of the LPF cutoff frequency in distributed coordination.

Using the LPF cutoff frequency as a coordination tool is also examined in this section, and the results are shown in Fig. 7. The maximum frequency deviation and the maximum power injected by the PHEVs, shown in Figs. 7(a) and (d), respectively, remain unchanged, as predicted in the previous section. The wind generator shaft torque and its derivative are depicted in Figs. 7(b) and (c), respectively. The results confirm that *flpf* can be used to control the mechanical tensions on the wind turbine shaft.

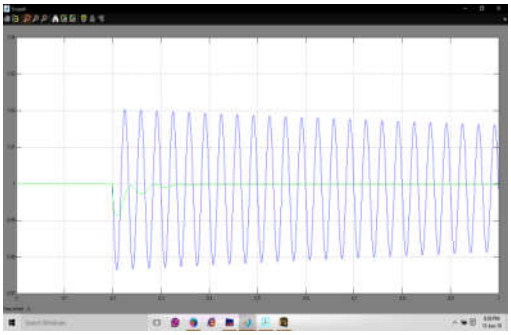

Fig:8(a) freq(p.u)

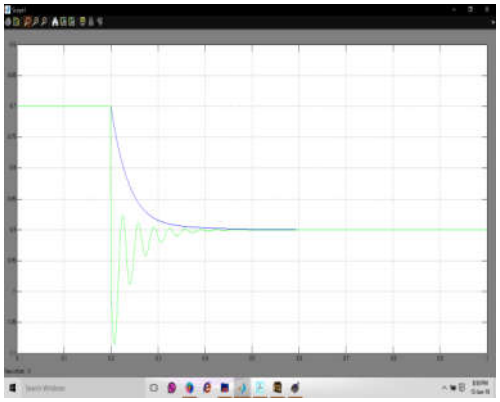

Fig:8(b) Ts(p.u)

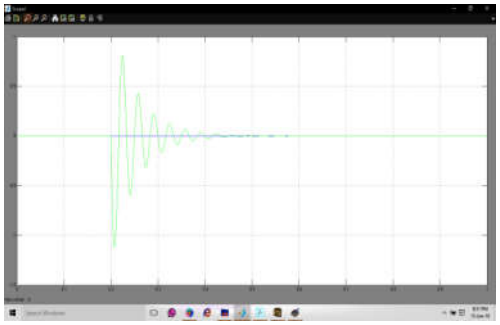

Fig:8(c) ROCOTs(pu)

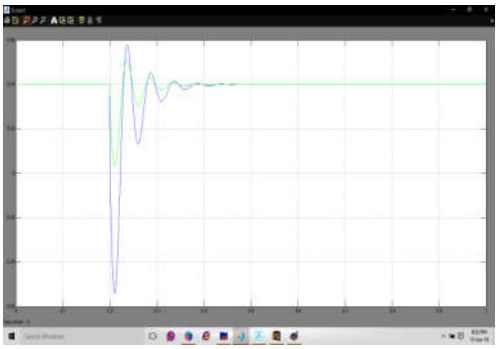

Fig:8(d) Pev(pu)

Fig:8. Simulation waveforms of Impact of unequal droop gains

Fig. 8 shows the case of unequal droop gains of the wind generator and the PHEVs. As predicted by the small-signal analysis, a much smaller PHEVs droop gain can make the system unstable. These results also confirm that instability happens only when *mp,phev* is a small fraction of the wind droop gain (less than one-fourth in the system under study). As shown in Figure, in the stable cases, a smaller PHEVs droop gain can amplify the mechanical tensions, particularly by affecting the rate of change of the shaft torque. On the other hand, when *mp,phev*/ *mp,wind* is higher than one, represented by the purple curves in Fig. 8, the system frequency dynamics and the ROCOT of the wind turbine shaft can be improved at the expense of higher power injection by the PHEVs. These results verify the arguments in the previous section: the distributed cooperative droop is robust against miscoordinations. In other words, it is not necessary to retune the control gains by any changes in PHEVs or wind available energy for frequency regulation. The proposed method can work effectively for a relatively large range of changes.

IV. CONCLUSION

With proper control and coordination, wind generators and PHEVs can compensate for each other's drawbacks and effectively participate in the primary frequency regulation of microgrids. The coordination mechanisms of these sources were investigated in this paper by using small-signal analysis and nonlinear time-domain simulations. The study showed the following. (1) The virtual inertia is not a suitable frequency regulation tool for the coordinated control. PHEVs do not benefit significantly from a coordinated virtual inertia, whereas the burden of the coordination is added to the system. (2) A centralized coordinated control for a droop is suitable either for a low contribution of wind-PHEVs combination to the frequency regulation or

in the presence of a very fast communication system. On the other hand, the distributed coordination does not perform very effectively when uncertainties about the wind and the PHEVs are very high. (3) A distributed control can guarantee the coordination and the LPF cutoff frequency can be used as the lever to manage the wind turbine mechanical tension while the PHEVs are regulated locally without needing a fast communication infrastructure.

REFERENCES

[1] "Global wind energy outlook," 2014 [Online]. Available: www.gwec.net.

[2] "Wind by Numbers: Economic Benefits of Wind Energy" from Canadian Wind Energy Association [Online]. Available: http://www.canwea.ca

[3] "New record-breaking year for Danish wind power", ENERGINET official Website, 2016.

[4] H. Polinder, F. van der Pijl, G.-J. de Vilder, P. J. Tavner, "Comparison of direct-drive and geared generator concepts for wind turbines," *IEEE Trans. Energy Convers*, vol.21, no.3, pp.725-733, Sept. 2006.

[5] N. Nguyen et. al., "An Analysis of the Effects and Dependency of Wind Power Penetration on System Frequency Regulation," *IEEE Trans. on Sustainable Energy*, vol. 7, no. 1, pp. 354-363, Jan. 2016.

[6] N. T. Janssen, et. al., "Frequency Regulation by Distributed Secondary Loads on Islanded Wind-Powered Microgrids," *IEEE Trans. on Sustainable Energy*, vol. 7, no. 3, pp. 1028-1035, July 2016.

[7] V. Knap; et. al., "Sizing of an Energy Storage System for Grid Inertial Response and Primary Frequency Reserve," *IEEE Trans. on Power Systems*, to be published.

[8] Liu, J. Wen, W. Yao and Y. Long, "Solution to short-term frequency response of wind farms by using energy storage systems," *IET Renewable Power Generation*, vol. 10, no. 5, pp. 669-678, 5 2016.

[9] F. Kennel, et. al., "Energy Management for Smart Grids With Electric Vehicles Based on Hierarchical MPC," *IEEE Trans. on Industrial Informatics*, vol. 9, no. 3, pp. 1528-1537, Aug. 2013.

[10] A. Nisar, et. al, "Comprehensive Control for Microgrid Autonomous Operation With Demand Response," *IEEE Trans. on Smart Grid*, to be published.